

Investigation of the Thermal Stability of High Energy Ball Milled SiC Nanoparticles Using Thermogravimetric and Differential Thermal Analysis

Manikandan Sekar^{1*}, Vinodhkumar Balakrishnan², Vivek Rajavelu³, Mohanram Parthiban³

¹ Department of Mechanical Engineering, National Institute of Technology, Karaikal, Puducherry-609 609, India

² Department of Agricultural Engineering, Shreenivasa Engineering College, Dharmapuri-635 301, Tamilnadu, India

³ Department of Mechatronics Engineering, K.S.Rangasamy College of Technology, Tiruchengode, Namakkal-637215, Tamil Nadu, India

* Corresponding author, e-mail: manikandan-jrf@nitpy.ac.in

Received: 19 November 2024, Accepted: 12 June 2025, Published online: 25 June 2025

Abstract

In this paper, an attempt has been made to analyze the thermal stability of silicon carbide (SiC) particles using thermogravimetric and differential thermal analysis (TGA/DTA). The SiC particles were made by using a high-energy ball milling (HEBM) process to break down micro-sized particles into nano-sized ones. The HEBM was conducted over 60 h, with samples collected at intervals of 15, 30, 45, and 60 h. The samples were further characterized using X-ray diffraction (XRD), scanning electron microscopy (SEM), and transmission electron microscopy (TEM) to examine changes in crystallinity and particle morphology. XRD analysis revealed shifts in peak positions, indicating structural changes induced by the milling process. SEM and TEM analyses showed a more homogeneous structure in the milled samples. TGA/DTA analysis demonstrated that nanosized SiC particles exhibited reduced thermal stability. Milling for a longer time caused mass loss to increase, ranging from 2% to 4.24%, at temperatures from 30 °C to 1000 °C and a heating rate of 20 °C/min in a nitrogen atmosphere. These findings show that nanosized SiC particles could be useful in high-temperature situations, especially in fields that need materials that are very stable at high temperatures.

Keywords

silicon carbide particles, high energy ball milling process, thermal stability, thermogravimetric analysis, characterization

1 Introduction

In recent years, the field of materials science has increasingly focused on nanostructured materials, with silicon carbide (SiC) nanoparticles emerging as a prominent area of interest due to their exceptional mechanical and thermal properties. Thermal stability is a critical property in assessing the performance and applicability of nano materials, particularly in high-temperature environments [1, 2]. The thermal behavior of these materials directly influences their structural integrity, functionality, and longevity in practical applications, ranging from electronics to aerospace engineering. Nanomaterials are defined by their high specific surface area (SSA), which gives them physical properties distinct from those of bulk materials [3]. Similarly, SiC exhibits unique functional properties at the nanoscale, including variations in melting point, corrosion resistance, electrical conductivity, and mechanical strength, compared to its bulk

form. SiC has exceptional physical properties, including high melting point (2700 °C), low density (3.21 g/cm³), high hardness (24 GPa), and a high elastic modulus (400 GPa) [1, 4]. It also exhibits excellent wear resistance, a low thermal expansion coefficient, high thermal conductivity, and strong oxidation resistance. Furthermore, SiC's ability to conduct heat, retain strength, and remain chemically stable in harsh environments and at high temperatures places it in a class above conventional material. Understanding the thermal stability of SiC nanoparticles is essential for practical applications, especially in settings where performance under extreme conditions is crucial [5, 6]. Fig. 1 [7] depicts the articles about synthesis of SiC and thermogravimetric and differential thermal analysis (TGA/DTA) [8–25]. The research conducted by Li and Sun [26] shows that gram-scale 3C-SiC nanoparticles can be produced from inexpensive 3C-SiC crystalline

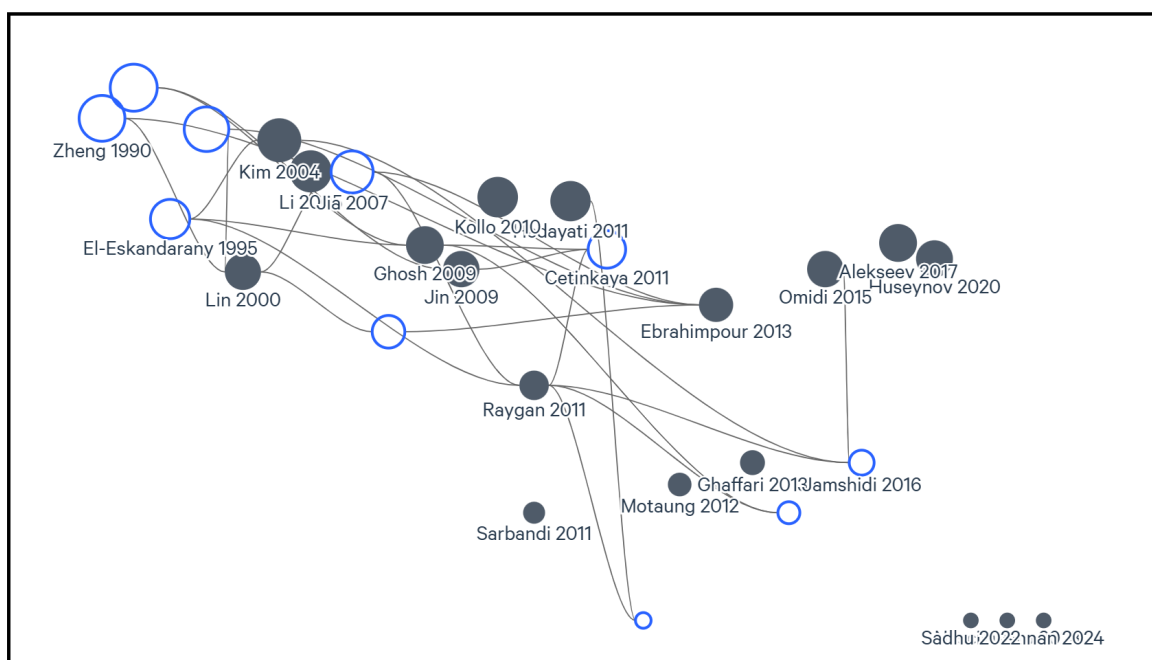


Fig. 1 Overview of articles on SiC synthesis and TGA/DTA analysis (Graph was prepared by Litmaps tool [7])

powder through a top-down ball-milling method for photocatalytic applications. The nanoparticles exhibit abundant surface states and an amorphous SiO_x shell, which effectively trap photogenerated electrons and prevent corrosion under visible light. Niu et al. [27] synthesized novel β -type SiC nanoparticles using a ball-milling method. The resulting nanoparticles included larger particles under 200 nm and smaller particles under 60 nm, produced from non-graphitizable carbon composed of carbon nanoparticles as the primary raw material. Kang et al. [28] studied the synthesis of SiC nanowires using high-energy ball milling (HEBM) of silicon and carbon powders, followed by annealing at 900 °C for 5 h and 1200 °C for 1 h. Madhusudan et al. [29] produced and characterized SiC nano powder from micron-sized SiC particles using a planetary-type ball mill. The ball milling (BM) process lasted up to 45 h, with toluene serving as a process control agent. The mass ratio of balls to powder remained fixed at 1:8 throughout the operation. Alexander Sivkov et al. [30] investigated the impact of arc discharge ignition methods on the effectiveness of precursor sublimation and the phase composition of the resulting ultra-dispersed product. The most effective way for plasma dynamic synthesis of β -SiC was to use thermal breakdown as the ignition mechanism. This method gave them yields of up to 99.9% of the product. The synthesized powder consisted of single-crystal particles with an average size of approximately 70 nm. Omidi et al. [31] developed a modified sol-gel method for synthesizing ultrafine SiC powders using tetraethoxysilane

and saccharose. The TGA was carried out at 1450 °C under nitrogen flow. Thermal analysis revealed mass loss around 200 °C due to saccharose decomposition and removal of unwanted components. Further thermal changes around 600 °C resulted in SiO_2 reduction. Huseynov et al. [2] study found that 3C-SiC nanocrystals have high surface activity, causing the hydroxyl or OH groups to gather on their surface. These groups completely remove from the surface at high temperatures, with groups O and H leaving the surface between 467 and 755 K, depending on the heating rate. At temperatures above 755 K, no OH groups are found. At a low heating rate of 5 K/min, OH groups completely leave the surface. Wang et al. [32] conducted a 10-h BM process on a SiC-composite coated with nickel nanoparticles, revealing that the addition of Ni nanoparticles significantly enhanced the thermal conductivity, hydrophobicity, thermal stability, and puncture resistance of the Aramid nanofiber composite film. A study by Liu and Yu [33] on SiC powder prepared using HEBM revealed that after 5 min of milling, the powder achieved a uniform particle size distribution, reduced particle diameters, and an increased SSA.

Recent advancements in nanoparticle fabrication methods, such as chemical vapor deposition and mechanical milling, have enabled precise tailoring of particle properties to suit diverse applications. Consequently, researchers [34–36] use various techniques to prepare SiC nanoparticles, but only a few have conducted characterization studies. Based on the available literature, it can be concluded that there is limited research on the production, characterization,

and thermal analysis of nanostructured particles using the HEBM process, particularly in the case of nanostructured SiC. Therefore, this paper aims to transform micro sized SiC into nanostructured SiC through HEBM and analyze the thermal stability of SiC at various milling durations.

By establishing a comprehensive profile of their thermal stability analysis, the study seeks to contribute valuable insights into their potential applications in high-temperature environments, thereby advancing the field of nanomaterial engineering and its related industries.

2 Materials and methods

SiC powder, with a minimum purity of 95% and initial particle size of 0.2 μm , was sourced from Himedia Chemicals PVT. Ltd., Mumbai, India. To reduce the SiC particle size from the micrometer to the nanometer scale, HEBM was performed using a Pulverisette 6, Classic Line planetary ball mill (Fritsch, Germany). Fig. 2 illustrates the

HEBM process used for the synthesis of SiC nanopowder. Mechanical milling has emerged as a critical technique for nanoparticle synthesis, significantly influencing their structural and functional properties. This method involves the physical attrition of materials, enabling particle size reduction to the nanoscale. Due to their small size, the resulting nanoparticles often exhibit an increased surface area and enhanced reactivity. In this study, the milling process was conducted in a steel jar using steel balls (10 mm diameter) as the milling media, maintaining a ball-to-powder mass ratio of 10:1 and a planetary carrier rotation speed of 400 rpm. The steel jar was first loaded with steel balls and SiC powder, then tightly sealed and securely mounted on the rotating element, following the manufacturer's instructions. Once the milling time and speed were set, the process was initiated. Samples were extracted every 15 h for analysis throughout the total milling duration of 60 h.

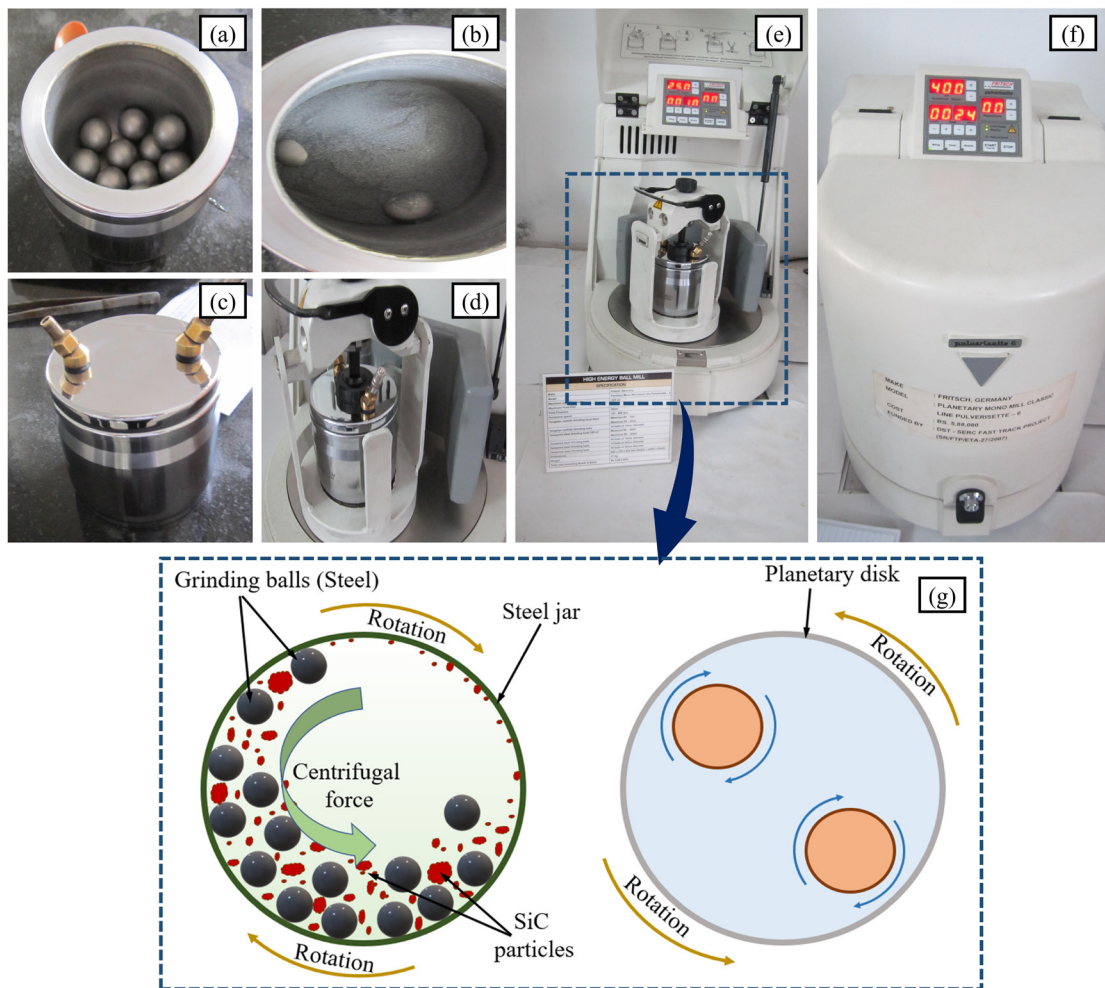


Fig. 2 High-energy ball milling process: (a) steel jar with balls, (b) addition of SiC powder, (c) sealed steel jar, (d) jar fitted in ball mill, (e) ball mill in open position, (f) ball mill in closed position, (g) ball milling working process [32]

3 Characterization of SiC particles

X-ray diffraction (XRD) patterns of mechanically milled SiC powder samples were recorded using a Bruker D8 Advance diffractometer with monochromatic Cu-K α 1 radiation (wavelength $\lambda = 1.5418 \text{ \AA}$). The diffraction was conducted at an accelerating voltage of 40 kV and a current of 20 mA to ensure optimal conditions for high-resolution measurements. This technique allows for the determination of the crystalline structure and phase composition of the SiC nanoparticles. In addition to XRD analysis, morphological studies were performed using scanning electron microscopy (SEM), specifically a Hitachi model, which offers magnification capabilities ranging from 5x to 300 000x. This range enables detailed observation of the surface morphology of the SiC nanoparticles. To facilitate elemental analysis, energy dispersive X-ray spectroscopy (EDAX) was integrated into the SEM setup, allowing for the identification and quantification of the elemental composition of the samples [37–39]. Furthermore, the morphology of the SiC powders was investigated using high-resolution transmission electron microscopy (HR-TEM) and selected area electron diffraction (SAED) on a JEM-2010 instrument operating at 200 kV. In this study, a thermogravimetric analyzer was utilized for thermal stability analysis. TGA and DTA were performed using a NETZSCH STA Jupiter 409 PL Luxx (Germany) thermal analysis instrument, which has an accuracy of 1%. The instrument was operated at a heating rate of 20 °C/min in a nitrogen atmosphere. Around 3 to 5 mg of each sample was placed in an alumina pan and heated from 30 °C to 1000 °C. The onset temperature of degradation and the residual mass were extracted from the resulting TGA/DTA curve. To assess measurement consistency, one sample was tested three times prior to measuring all the samples. Mass loss exhibited repeatability and reproducibility within $\pm 0.1\%$, while the onset temperatures of thermal events varied within $\pm 12 \text{ }^\circ\text{C}$.

4 Result and discussion

The XRD pattern of SiC samples, both before the milling process and after milling for durations of 15, 30, 45, and 60 h, is shown in Fig. 2. The XRD pattern displays diffraction peaks corresponding to specific lattice planes in the SiC crystal structure. These peaks are labeled with their Miller indices, a set of three integers (hkl) that uniquely identify crystallographic planes. In this study, the peaks observed at $2\theta = 35.52^\circ$, 37.31° , 60.02° , 71.83° , and 75.56° correspond to the (111), (200), (220), (311), and (222) reflections of SiC, respectively, as indexed in JCPDS

file No. 29-1129 and previous studies [40–42]. The crystallite size was calculated from the XRD patterns using the Scherrer equation. The resulting sizes were 212, 142, 106, 54, and 35.4 nm for milling durations of 0, 15, 30, 45, and 60 h, respectively. In comparison with unmilled samples, the XRD peaks for various hours-milled samples are broad due to the reduction in SiC particle size (see Fig. 3). Thus, HEBM increases the amorphous phase of SiC by decreasing the crystallinity. Fig. 4(a–f) presents SEM and TEM images of unmilled and milled SiC particles. Figs. 4(a) and 4(b) show the SEM images for different magnifications of the unmilled SiC particles, where it can be observed that the agglomerates in these samples exhibit highly irregular angular shapes. Figs. 4(c) and 4(d) display SEM images of SiC particles after 60 h of milling, shown at different magnifications. It can be observed that the particles are agglomerated and reduced to nanometer sizes, with their shapes appearing sub-angular. Table 1 presents the EDX analysis results of the milled (60 h) SiC particles, confirming the presence of silicon and carbon, which indicates the formation of SiC. Moreover, some iron particles were detected in the analysis, likely due to contamination from the steel jar and balls used as the milling media.

TEM and SAED analyses were conducted to examine the morphology and microstructure of the SiC particles after 60 h of milling. Figs. 4(e) and 4(f) reveals that the SiC

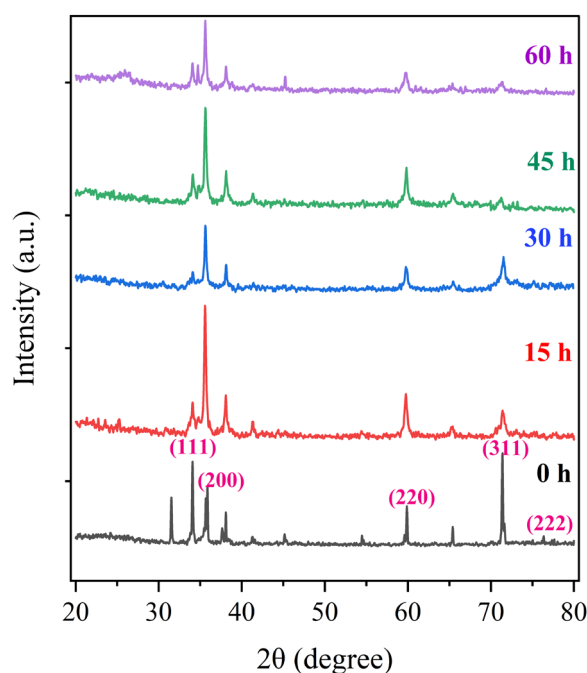


Fig. 3 Comparison of XRD patterns of unmilled and milled SiC samples

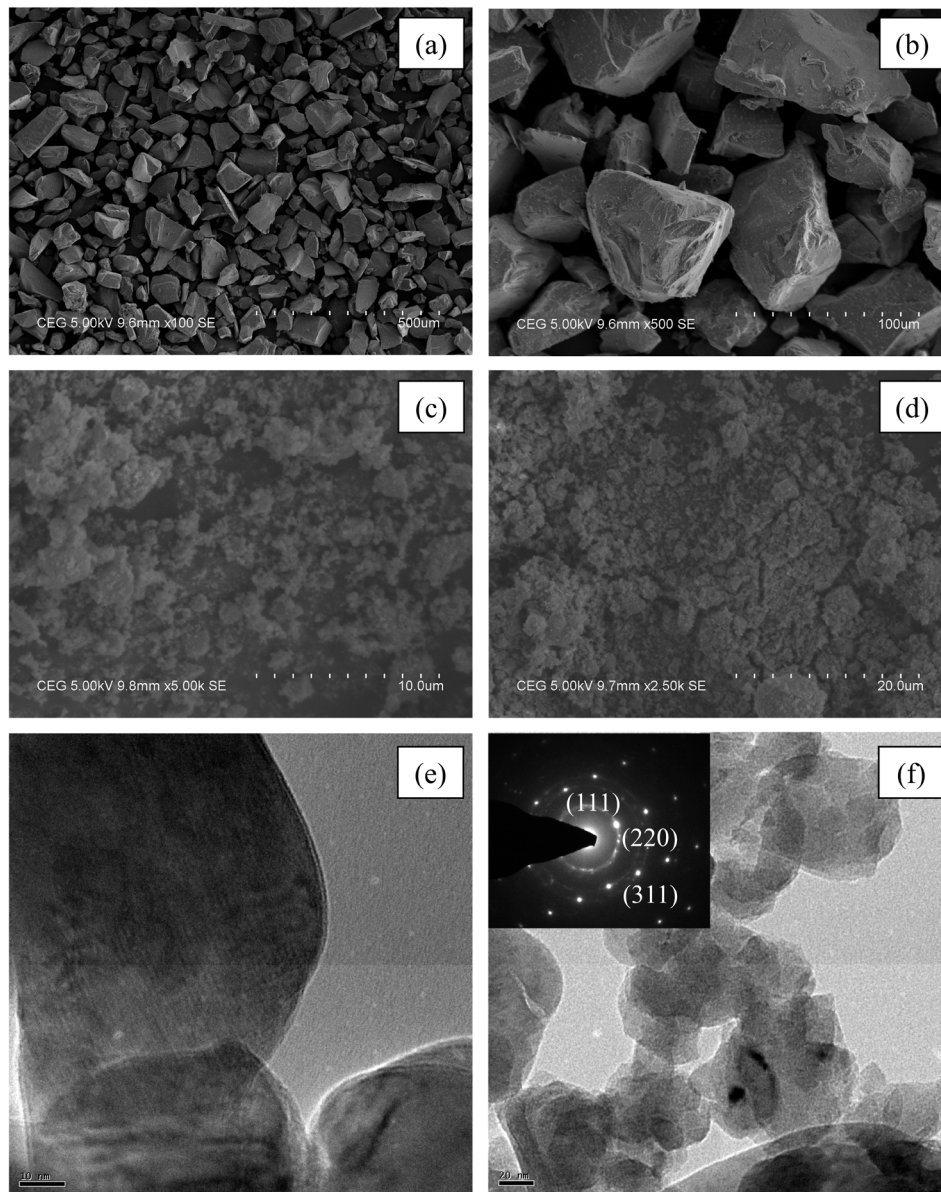


Fig. 4 SEM and TEM images at different magnifications: (a) SEM images of unmilled SiC particles (100x magnification) and (b) SEM images of unmilled SiC particles (500x magnification); (c) SEM images of SiC particles milled for 60 h (5000x magnification) and (d) SEM images of SiC particles milled for 60 h 2500x magnification; (e) TEM images of SiC particles milled for 60 h without the corresponding SAED pattern and (f) TEM images of SiC particles milled for 60 h with the corresponding SAED pattern

Table 1 EDAX analysis of SiC

Element	Mass %	Atom %
C	6.79	11.54
Si	89.53	86.67
Fe	3.68	1.79
Total	100	100

powders synthesized after 60 h consist of agglomerates with sub-angular shapes, varying in size from 10 to 100 nm. The SAED pattern in Fig. 4(f) shows three distinct polycrystalline rings, indexed as (111), (220), and (311) for SiC.

These rings match the XRD results, confirming the presence of SiC and indicating that the particles are in an amorphous phase [43]. This alignment of SAED and XRD results strongly supports that, despite the nanoscale structure, the SiC retains its crystallographic integrity as polycrystalline SiC, highlighting the success of the milling process in producing amorphous, nanoscale SiC.

The study examines the thermal stability of SiC particles, which have been milled for different durations, and their results are presented in Fig. 5(a)-(e). The analysis was conducted across a temperature range of 30 °C to 1000 °C,

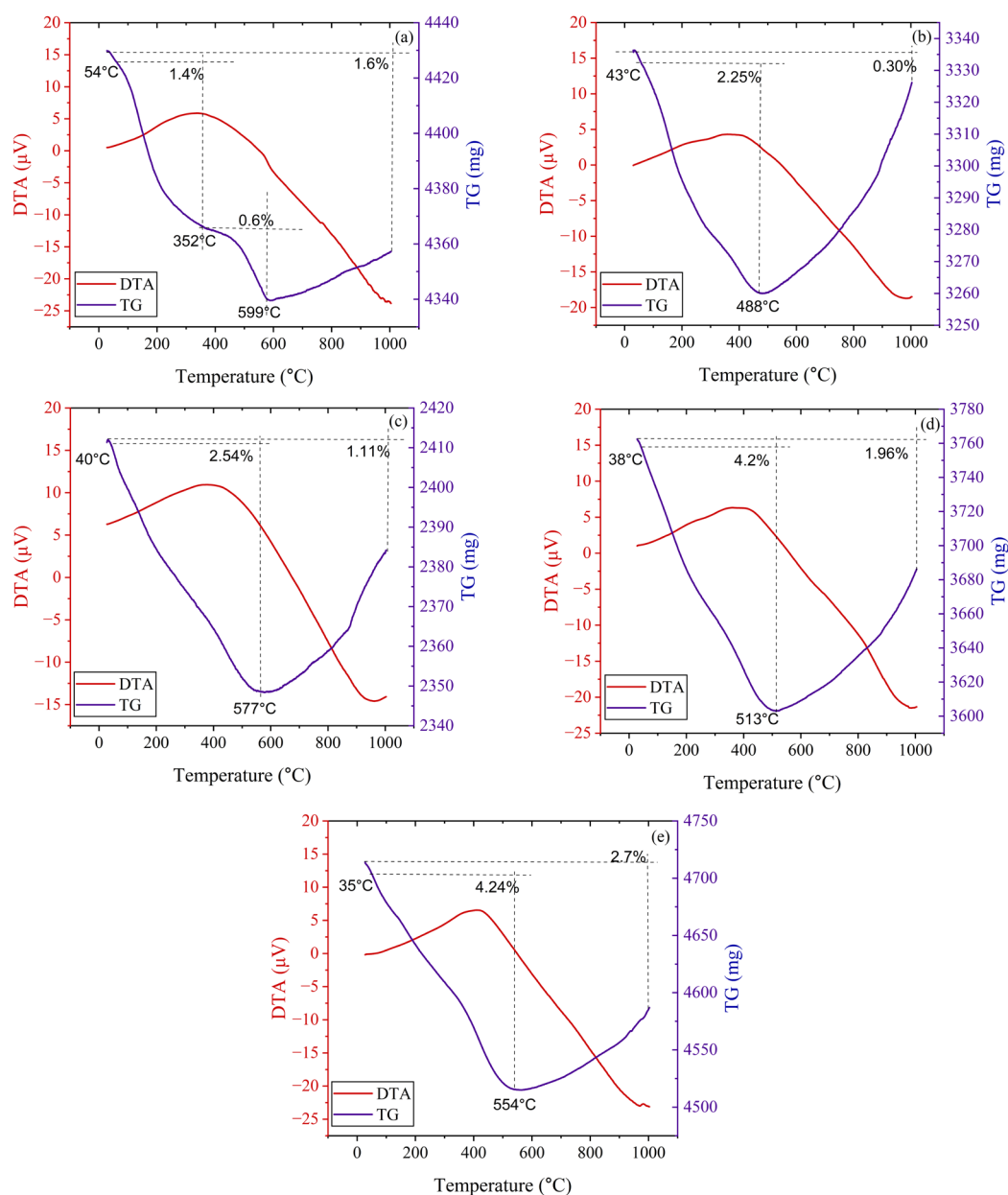


Fig. 5 TGA/DTA curves for (a) unmilled SiC particles, (b) SiC particles milled for 15 h, (c) SiC particles milled for 30 h, (d) SiC particles milled for 45 h, and (e) SiC particles milled for 60 h

with a heating rate of 20 °C/min, in a nitrogen atmosphere. The results show that unmilled and milled SiC particles exhibit moderate thermal stability and limited mass loss due to their resistance to evaporation and phase changes. The TGA and DTA curves show the change in mass of the sample and the temperature difference between the sample and a reference material, with upward peaks representing exothermic reactions and downward peaks representing endothermic reactions [44, 45].

Fig. 5(a) depicts the TGA and DTA curves of unmilled SiC particles with a heating rate of 20 °C/min. From the TGA curve, it can be observed that between 54 °C and 352 °C,

there is a small mass loss of 1.4%, likely due to the release of adsorbed moisture or surface-bound volatile components. Between 352 °C and 599 °C, an additional mass loss of 0.6% occurs, which may be associated with the decomposition of organic residues or surface oxides. In the temperature range of 600 °C to 1000 °C, the mass percentage goes up by a small amount, up to 0.5%. This could be because of trace impurities or oxygen that is still in the nitrogen atmosphere, which causes some oxidation and the creation of a protective SiO₂ layer on the surface of the SiC. The DTA curve indicates the thermal events occurring in the sample, such as endothermic or exothermic reactions. A small

endothermic peak is seen around 352 °C, which could be due to moisture loss or minor decomposition. Between 352 °C and 599 °C, a bigger event could be a phase transition or the continued breakdown of surface impurities. Further, from 599 °C to 1000 °C shows a continuous downward trend, indicating an endothermic process.

Fig. 5(b) shows the TGA/DTA curve for SiC particles milled for 15 h. In the TGA curve, a small mass loss of 0.30% is noted at high temperatures, suggesting minor decomposition or the release of volatile substances. The 2.25% mass loss around 488 °C indicates a significant event, probably brought on by the thermal decomposition of a component in the SiC sample. Within the temperature range of 488 °C to 1000 °C, there is a minor increase in the mass percentage, reaching 1.95%. This could be because of small amounts of oxygen left in the nitrogen atmosphere or impurities, which cause some oxidation and the creation of a protective SiO₂ layer on the surface of the SiC. In the same way, the DTA curve has a peak around 488 °C, which means an endothermic event happened. This could be a phase change, decomposition, or another endothermic reaction in the sample. The small peak near 43 °C suggests a minor thermal event, possibly due to moisture evaporation or a low-temperature phase transition.

Fig. 5(c) shows the TGA/DTA curves for SiC particles milled for 30 h. In the TGA curve, a small mass loss of 1.11% is observed at high temperatures, likely indicating the release of volatile compounds. A more significant mass loss of 2.54% occurs around 577 °C, suggesting major thermal decomposition or the loss of a component in the sample. The mass percentage increases to 1.43% between 577 °C and 1000 °C when the SiC undergoes partial oxidation and a protective SiO₂ layer forms on its surface. This could be because of trace impurities or residual oxygen in the nitrogen atmosphere. The DTA curve shows a peak at 577 °C, indicating an endothermic event that could correspond to a phase change, decomposition, or another endothermic reaction. Also, a minor peak near 40 °C suggests a small thermal event, possibly due to moisture evaporation or a low-temperature phase transition.

Fig. 5(d) shows the TGA/DTA curves for SiC particles milled for 45 h. In the TGA curve, a mass loss of 1.96% is observed at high temperatures, possibly due to the release of volatile compounds. A more significant mass loss of 4.2% occurs around 513 °C, suggesting major thermal decomposition or the breakdown of a component within the sample. Between 513 °C and 1000 °C, when the mass percentage rises slightly to 2.24%, SiC may go through some oxidation and form a protective SiO₂ layer on its

surface. This could be because of trace impurities or residual oxygen in the nitrogen atmosphere. The DTA curve has a peak around 513 °C, which means that there was an endothermic reaction in the sample, most likely because of a phase change, decomposition, or some other endothermic event. Moreover, a smaller peak near 38 °C may correspond to a minor thermal event, such as moisture evaporation or a low-temperature phase transition.

Fig. 5(e) presents the TGA/DTA curves for SiC particles milled for 60 h. In the TGA curve, a significant mass loss of 4.24% occurs around 554 °C, signifying the thermal decomposition or breakdown of a component within the sample. The mass percentage goes up to 1.7% between 554 and 1000 °C.

This might be because of small impurities or oxygen that is still in the nitrogen atmosphere. This oxygen causes some oxidation and the formation of a protective SiO₂ layer on the SiC surface. The DTA curve shows a peak near 426 °C, indicating an endothermic reaction likely associated with a phase change, decomposition, or another endothermic event. Additionally, a smaller peak near 35 °C may correspond to a minor thermal event, such as moisture evaporation or a low-temperature phase transition. Table 2 presents the percentage mass loss for various milling durations in TGA analysis. The first column represents the milling duration, ranging from 0 to 60 h. The second column indicates the percentage of material lost during milling, while the third column represents the corresponding temperature. Initially (0 h), the mass loss is 2% at a temperature of 599 °C. As milling progresses, the mass loss gradually increases, reaching a maximum of 4.24% at 60 h. The temperature fluctuates rather than following a linear trend, with values ranging from 488 °C to 599 °C. These data indicate that prolonged milling generally leads to increased mass loss, as high-energy grinding breaks down particles and may result in the loss of volatile components or surface material. Extended BM of SiC nanoparticles can reduce thermal stability due to the increased surface area, which introduces more surface defects and increases the likelihood of oxidation or reactions with the surrounding environment, ultimately diminishing the material's thermal resistance.

Table 2 Mass loss for various milling hours & TGA analysis

Milling duration (h)	Mass loss (%)	Temperature (°C)
0	2	599
15	2.25	488
30	2.54	577
45	4.20	513
60	4.24	554

The sintering onset temperatures shown in Table 2 do not follow a consistent increasing or decreasing trend with milling duration. From the Table 2 found that the unmilled SiC (0 h) begins sintering at 599 °C, but after 15 h of milling, the temperature significantly drops to 488 °C. With 30 h of milling, the onset temperature rises again to 577 °C, then decreases to 513 °C at 45 h, and increases once more to 554 °C at 60 h. This irregular behavior indicates no clear trend in the sintering onset temperature with increasing milling time. Such fluctuations may be attributed to inconsistent microstructural changes during milling, as well as variations in surface defects and reactivity. Fig. 5(a)-(e) illustrates the remarkable changes in the thermal stability of SiC, with minimal mass loss observed even at higher temperatures up to 599 °C and beyond, regardless of the milling duration that transforms the material from micro to nanosized particles. This consistent behavior highlights the inherent thermal resilience of SiC, making it an excellent for applications where high-temperature resistance and durability against thermal degradation are essential. Such stability ensures that SiC can maintain its structural integrity in extreme conditions, reinforcing its value in industries that demand reliable performance at elevated temperatures.

5 Conclusion

The SiC nanoparticles were synthesized using a HEBM process, and their thermal stability was studied. The

XRD patterns confirmed the crystallinity of the SiC particles, while SEM and TEM analyses revealed the morphology of the nanoparticles as irregular angular shapes. The findings of this investigation into the thermal stability of mechanically milled SiC nanoparticles highlight the significant influence of milling duration on thermal behavior, as evidenced by TGA/DTA analysis conducted from 30 °C to 1000 °C at a heating rate of 20 °C/min in a nitrogen atmosphere. The observed mass loss percentages were 2.00%, 2.25%, 2.54%, 4.20%, and 4.24%, corresponding to milling durations of 0, 15, 30, 45, and 60 h, respectively. DTA analysis revealed both endothermic and exothermic processes under these conditions. The results demonstrate that prolonged milling enhances the surface area, leading to changes in the degradation dynamics of SiC. This underscores the critical interplay between mechanical processing and thermal stability. Additionally, DTA analysis showed significant shifts in phase transformation temperatures, which are crucial for applications requiring high-temperature performance. This study not only advances our understanding of SiC nanoparticles but also provides a foundation for future research aimed at optimizing milling parameters for specific engineering applications. The implications of this research extend beyond the laboratory, suggesting pathways for developing advanced materials that harness the unique properties of SiC, thereby driving innovation in various engineering fields for high-temperature applications.

References

- [1] Wang, Y., Dong, S., Li, X., Hong, C., Zhang, X. "Synthesis, properties, and multifarious applications of SiC nanoparticles: A review", *Ceramics International*, 48(7), pp. 8882–8913, 2022. <https://doi.org/10.1016/j.ceramint.2021.12.208>
- [2] Huseynov, E. M., Naghiyev, T. G. "Various thermal parameters investigation of 3C-SiC nanoparticles at the different heating rates", *Applied Physics A*, 128(2), 115, 2022. <https://doi.org/10.1007/s00339-022-05265-x>
- [3] Kostoglou, N., Stock, S., Solomi, A., Holzapfel, D. M., Hinder, S., ..., Mitterer, C. "The Roles of Impurities and Surface Area on Thermal Stability and Oxidation Resistance of BN Nanoplatelets", *Nanomaterials*, 14(7), 601, 2024. <https://doi.org/10.3390/nano14070601>
- [4] Zhang, W. "An overview of the synthesis of silicon carbide-boron carbide composite powders", *Nanotechnology Reviews*, 12(1), 20220571, 2023. <https://doi.org/10.1515/ntrev-2022-0571>
- [5] Zeng, G., Huang, X., Li, J., Yue, J., Zhang, H., Tang, X.-Z. "Multifunctional SiC/C hybrid fabric applicable for extreme environment ranging from liquid nitrogen temperature to 1000 °C", *Ceramics International*, 49(7), pp. 10889–10896, 2023. <https://doi.org/10.1016/j.ceramint.2022.11.282>
- [6] Zhu, S., Zhang, G., Bao, Y., Sun, D., Zhang, Q., Meng, X., Hu, Y., Yan, L. "Progress in preparation and ablation resistance of ultra-high-temperature ceramics modified C/C composites for extreme environment", *Reviews on Advanced Materials Science*, 62(1), 20220276, 2023. <https://doi.org/10.1515/rams-2022-0276>
- [7] Litmaps "Litmaps, (Version 2025-01-16)", [computer program] Available at: <https://app.litmaps.com/> [Accessed: 18 June 2025]
- [8] Li, X., Wang, X., Bondokov, R., Morris, J., An, Y. H., Sudarshan, T. S. "Micro/nanoscale mechanical and tribological characterization of SiC for orthopedic applications", *Journal of Biomedical Materials Research*, 72B(2), pp. 353–361, 2005. <https://doi.org/10.1002/jbm.b.30168>
- [9] Lin, Y.-J., Chen, L.-J. "Oxidation of SiC powders in SiC/alumina/zirconia compacts", *Ceramics International*, 26(6), pp. 593–598, 2000. [https://doi.org/10.1016/S0272-8842\(99\)00102-9](https://doi.org/10.1016/S0272-8842(99)00102-9)
- [10] Ebrahimpour, O., Chaouki, J., Dubois, C. "Diffusional effects for the oxidation of SiC powders in thermogravimetric analysis experiments", *Journal of Material Science*, 48(12), pp. 4396–4407, 2013. <https://doi.org/10.1007/s10853-013-7258-0>

- [11] Huseynov, E., Naghiyev, T. G., Aliyeva, U. S. "Thermal parameters investigation of neutron-irradiated nanocrystalline silicon carbide (3C–SiC) using DTA, TGA and DTG methods", *Physica B: Condensed Matter*, 577, 411788, 2020.
<https://doi.org/10.1016/j.physb.2019.411788>
- [12] Kollo, L., Leparoux, M., Bradbury, C. R., Jäggi, C., Carreño-Morelli, E., Rodriguez-Arbaizar, M. "Investigation of planetary milling for nano-silicon carbide reinforced aluminium metal matrix composites", *Journal of Alloys and Compounds*, 489(2), pp. 394–400, 2010.
<https://doi.org/10.1016/j.jallcom.2009.09.128>
- [13] Ghosh, B., Pradhan, S. K. "Microstructural characterization of nanocrystalline SiC synthesized by high-energy ball-milling", *Journal of Alloys and Compounds*, 486(1–2), 2009, pp. 480–485, 2009.
<https://doi.org/10.1016/j.jallcom.2009.06.170>
- [14] Kim, I.-S., Blomgren, G. E., Kumta, P. N. "SiC nanocomposite anodes synthesized using high-energy mechanical milling", *Journal of Power Sources*, 130(1), pp. 275–280, 2004.
<https://doi.org/10.1016/j.jpowsour.2003.12.014>
- [15] Raygan, S., Kondori, B., Yangijeh, H. M. "Effect of Mechanical Activation on the Production of SiC from Silica Sand", *International Journal of Refractory Metals and Hard Materials*, 29(1), pp. 10–13, 2011.
<https://doi.org/10.1016/j.ijrmhm.2010.06.002>
- [16] Hedayati, M., Salehi, M., Bagheri, R., Panjepour, M., Maghziyan, A. "Ball Milling Preparation and Characterization of Poly (Ether Ether Ketone)/Surface Modified Silica Nanocomposite", *Powder Technology*, 207(1–3), pp. 296–303, 2011.
<https://doi.org/10.1016/j.powtec.2010.11.011>
- [17] Jin, H.-B., Li, J.-T., Cao, M.-S., Agathopoulos, S. "Influence of Mechanical Activation on Combustion Synthesis of Fine Silicon Carbide (SiC) Powder", *Powder Technology*, 196(2), pp. 229–232, 2009.
<https://doi.org/10.1016/j.powtec.2009.07.016>
- [18] Omidi, Z., Ghasemi, A., Bakhshi, S. R. "Synthesis and Characterization of SiC Ultrafine Particles by Means of Sol-Gel and Carbothermal Reduction Methods", *Ceramics International*, 41(4), pp. 5779–5784, 2015.
<https://doi.org/10.1016/j.ceramint.2015.01.005>
- [19] Sarbandi, M. R. "Study of the influence of nanoparticles on the performance and the properties of polyamide 6", PhD Thesis, University Stuttgart, 2011.
<https://doi.org/10.18419/opus-1342>
- [20] Motaung, T. E., Luyt, A. S., Bondioli, F., Messori, M., Saladino, M. L., Spinella, A., Nasillo, G., Caponetti, E. "PMMA–Titania Nanocomposites: Properties and Thermal Degradation Behaviour", *Polymer Degradation and Stability*, 97(8), pp. 1325–1333, 2012.
<https://doi.org/10.1016/j.polymdegradstab.2012.05.022>
- [21] Sadhu, K. K., Mandal, N., Sahoo, R. R., Sadhu, K. K., Mandal, N., Sahoo, R. R. "Effect of Ball Milling Mechanism on the Density and Hardness of Al Matrix Consolidated Through Pressure Less Sintering", In: *Advances in Micro and Nano Manufacturing and Surface Engineering*, Proceedings of AIMTDR 2021, Kanpur, India, 2021, pp. 283–289. ISBN: 978-981-19-4571-7
https://doi.org/10.1007/978-981-19-4571-7_25
- [22] Ghaffari, S., Alizadeh, M., Asadian, K., Ebadzadeh, T., Ghanbari, A. "Effects of milling and subsequent heat treatment on preparation of mullite–zirconia nanocomposites", *Micro & Nano Letters*, 8(4), pp. 193–196, 2013.
<https://doi.org/10.1049/mnl.2013.0008>
- [23] Krishnan, M. N., Suresh, S., Prema, C. E. "Enhanced Performance of Mg (AZ91) Composites with Nano B₄C: A Comprehensive Study of Microstructure, Mechanical Properties, Acoustic Emission and Thermogravimetric Analysis", *Transactions of the Indian Institute of Metals*, 77(11), pp. 3557–3572, 2024.
<https://doi.org/10.1007/s12666-024-03412-x>
- [24] Nascimento, L., de Melo Costa, A. C. F. "Synthesis by Mechanical Alloying and Characterization Fe₇₃Si₂₂B₅ Alloy: Amorphization Evaluation", *Brazilian Journal of Physics*, 53(6), 158, 2023.
<https://doi.org/10.1007/s13538-023-01371-0>
- [25] Alekseev, S., Shamatulskaya, E., Volvach, M., Gryn, S., Korytko, D., Bezverkhyy, I., Iablokov, V., Lysenko, V. "Size and Surface Chemistry Tuning of Silicon Carbide Nanoparticles", *Langmuir*, 33(47), pp. 13561–13571, 2017.
<https://doi.org/10.1021/acs.langmuir.7b02784>
- [26] Li, H., J. Sun, J. "Highly Selective Photocatalytic CO₂ Reduction to CH₄ by Ball-Milled Cubic Silicon Carbide Nanoparticles under Visible-Light Irradiation", *ACS Applied Materials & Interfaces*, 13(4), pp. 5073–5078, 2021.
<https://doi.org/10.1021/acsami.0c19945>
- [27] Niu, J., Wang, Z., Liu, H., Ma, Y., Pang, H., Wang, X. "Synthesis of silicon carbide nanoparticles from amorphous carbon: Based on the domain structure of electrically calcined anthracite", *Ceramics International*, 49(18), pp. 29542–29552, 2023.
<https://doi.org/10.1016/j.ceramint.2023.06.147>
- [28] Kang, P., Zhang, B., Wu, G., Gou, H., Chen, G., Jiang, L., Mula, S. "Synthesis of β-SiC nanowires by ball milled nanoparticles of silicon and carbon", *Journal of Alloys and Compounds*, 604, pp. 304–308, 2014.
<https://doi.org/10.1016/j.jallcom.2014.03.011>
- [29] Madhusudan, B. M., Raju, H. P., Ghanaraja, S., Sudhakar, G. N. "Study of Microstructure and Mechanical Properties of Ball milled Nano-SiC Reinforced Aluminium Matrix Composites", *Journal of The Institution of Engineers (India): Series D*, 102(1), pp. 167–172, 2021.
<https://doi.org/10.1007/s40033-021-00257-2>
- [30] Sivkov, A., Nikitin, D., Shanenkov, I., Ivashutenko, A., Rahmatullin, I., Nassyrbayev, A. "Optimization of plasma dynamic synthesis of ultradispersed silicon carbide and obtaining SPS ceramics on its basis", *International Journal of Refractory Metals and Hard Materials*, 79, pp. 123–130, 2019.
<https://doi.org/10.1016/j.ijrmhm.2018.11.016>
- [31] Su, X., Zhou, W., Xu, J., Wang, J., He, X., Fu, C. "Preparation and dielectric property of B and N-codoped SiC powder by combustion synthesis", *Journal of Alloys and Compounds*, 551, pp. 343–347, 2013.
<https://doi.org/10.1016/j.jallcom.2012.10.153>

- [32] Wang, X., Dong, H., Ma, Q., Chen, Y., Zhao, X., Chen, L. "Nickel nanoparticle decorated silicon carbide as a thermal filler in thermal conductive aramid nanofiber-based composite films for heat dissipation applications", *RSC Advances*, 13(30), pp. 20984–20993, 2023.
<https://doi.org/10.1039/d3ra03336h>
- [33] Liu, G., Yu, H. "Characterization of mechanochemical modification in SiC powder", *Journal of Dispersion Science and Technology*, 2024.
<https://doi.org/10.1080/01932691.2024.2333522>
- [34] Srinivasa Perumal, K. P., Selvarajan, L., Mathan Kumar, P., Shriguppikar, S. "Enhancing mechanical and morphological properties of glass fiber reinforced epoxy polymer composites through rutile nanoparticle incorporation", *Progress in Additive Manufacturing*, 10(1), pp. 831–848, 2024.
<https://doi.org/10.1007/s40964-024-00675-0>
- [35] Heidarinassab, S., Nyabadza, A., Ahad, I. U., Brabazon, D. "Investigation of ablation efficiency and properties of silicon carbide nanoparticles synthesised using pulsed laser ablation in liquid", *Optics and Lasers Engineering*, 180, 108341, 2024.
<https://doi.org/10.1016/J.OPTLASENG.2024.108341>
- [36] Suresh, N., Balamurugan, L., Jayabalakrishnan, D. "Influence of SiC and WC reinforcements on the mechanical characteristics of AA6061 hybrid metal matrix composites", *Proceedings of the Institution of Mechanical Engineers, Part E: Journal of Process Mechanical Engineering*, 237(3), pp. 955–970, 2023.
<https://doi.org/10.1177/09544089221141353>
- [37] Manikandan, S., Nanthakumar, A. J. D. "Experimental Study of Cu Nanoparticles Loading and Temperature Effects on the Thermophysical Properties of SAE10W oil: Developing a New Mathematical Correlation", *Periodica Polytechnica Chemical Engineering*, 68(2), pp. 216–229, 2024.
<https://doi.org/10.3311/PPCh.23140>
- [38] Manikandan, S., Nanthakumar, A. J. D. "Predicting Dynamic Viscosity in Nanofluids of Graphene Nanoplatelets and SAE10W Oil Utilizing Artificial Neural Networks", *Periodica Polytechnica Chemical Engineering*, 68(4), pp. 571–581, 2024.
<https://doi.org/10.3311/PPCh.37179>
- [39] Manikandan, S., Nanthakumar, A. J. D. "Experimental Investigation and Specific Heat Capacity Prediction of Graphene Nanoplatelet-Infused SAE10W Oil Using Artificial Neural Networks", *Periodica Polytechnica Chemical Engineering*, 68(3), pp. 437–445, 2024.
<https://doi.org/10.3311/PPCh.37050>
- [40] Kim, K. J., Lee, S., Lee, J. H., Roh, M. H., Lim, K. Y., Kim, Y. W. "Structural and optical characteristics of crystalline silicon carbide nanoparticles synthesized by carbothermal reduction", *Journal of the American Ceramic Society*, 92(2), pp. 424–428, 2009.
<https://doi.org/10.1111/j.1551-2916.2008.02913.x>
- [41] Rao, J., Catherin, G., Murthy, I., Rao, D., Raju, B. "Production of nano structured silicon carbide by high energy ball milling", *International Journal of Engineering, Science and Technology*, 3(4), pp. 82–88, 2011.
<https://doi.org/10.4314/ijest.v3i4.68544>
- [42] Manikandan, S., Jancirani, J. "A study of preparation and characterization of nano-sized SiC powder using high energy ball milling", *Applied Mechanics and Materials*, 592–594, pp. 13–17, 2014.
<https://doi.org/10.4028/www.scientific.net/AMM.592-594.13>
- [43] Liu, R., Liu, M., Chang, J. "Large-scale synthesis of monodisperse SiC nanoparticles with adjustable size, stoichiometric ratio and properties by fluidized bed chemical vapor deposition", *Journal of Nanoparticle Research*, 19(2), 26, 2017.
<https://doi.org/10.1007/s11051-016-3737-y>
- [44] Huseynov, E. M., Naghiyev, T. G. "Study of thermal parameters of nanocrystalline silicon carbide (3C-SiC) using DSC spectroscopy", *Applied Physics A*, 127(4), 267, 2021.
<https://doi.org/10.1007/s00339-021-04410-2>
- [45] Akbarpour, M. R., Gazani, F., Mirabad, H. M., Khezri, I., Moeini, A., Sohrabi, N., Kim, H. S. "Recent advances in processing, and mechanical, thermal and electrical properties of Cu-SiC metal matrix composites prepared by powder metallurgy", *Progress in Materials Science*, 140, 101191, 2023.
<https://doi.org/10.1016/j.pmatsci.2023.101191>